

Design of an Invasive Blood Pressure (IBP) Monitoring System

A Report Submitted in Partial Fulfillment of the Requirements for
SYDE 362

Josh Bradshaw, 20479758, 3B

Sarah Cook, 20465516, 3B

Matt Jones, 20474981, 3B

Isaac Hunter, 20480938, 3B

Faculty of Engineering
Department of Systems Design Engineering

March 31, 2016

Course Instructor: Professor J. Kofman

Abstract

A low cost device for performing real-time direct arterial blood pressure measurements was designed for use in preclinical studies at the Hospital for Sick Children. The principal design challenge was designing an MRI compatible amplifier for used with the Transpac IV blood pressure transducer. The system was required to conform to a large variety of MRI safety standards:, as well as operating room sterility requirements. Analysis was carried out to minimize the effects of the MRI scanner's high power electromagnetic noise output on the amplifier, and to determine the amount of pressure attenuation caused by extending the invasive blood pressure line out of the MRI scanner's bore. The system's accuracy was tested using bench-top models, and it was field tested in a three hour animal experiment at the Hospital for Sick Children. The system outperformed three commercially available systems in terms of accuracy and noise immunity, and it costs 90% less than the least expensive commercial alternative. Future work includes designing an integrated system to replace the electronic test equipment that was used in prototype testing, and building medical grade enclosures for the components.

Contents

1	Introduction	1
1.1	Background on MRI and Gated Acquisition	1
1.1.1	Overview the MRI Environment	2
1.1.2	Hazards of the MRI Environment	3
1.2	State of the Art	4
1.2.1	Samba Preclin - \$11,500 CAD	4
1.2.2	Transonic Ultrasonic - \$10,200 CAD	4
1.2.3	SA Instruments - \$17,000 CAD	5
1.2.4	Limitations of Existing Methods	5
1.3	Design Statement	5
1.3.1	Statement of Need	5
1.3.2	Problem Definition	6
1.4	Previous Work	6
1.5	Project Goals and Objectives	6
1.6	Expected Impact	7
2	Requirements and Specifications	8
2.1	Design Requirements	8
2.1.1	Medical Device Sterility Requirements	8
2.1.2	Functional Requirements	8
2.1.3	User Requirements	9
2.1.4	Engineering Requirements	9
2.1.5	Mechanical Constraints	10
2.1.6	MRI Compatibility Requirements	10
2.2	Overview of Design Solution	11
3	Engineering Analysis	13
3.1	Circuit Design Overview	13

3.1.1	Electromagnetic Interference Analysis	13
3.1.2	Transpac IV Analysis	14
3.1.3	Amplifier Selection	15
3.1.4	EMI Input Filter Design	15
3.1.5	Cable Driver Amplifier	19
3.1.6	Power Supply Filter	19
3.1.7	Cable Selection	21
3.1.8	Bridge Driver	21
3.1.9	PCB Design for MRI Compatibility	22
3.2	Shielding Analysis and Design	22
3.2.1	Mathematical Model	22
3.2.2	Material Selection	23
3.2.3	Minimum Shield Thickness Calculation	23
3.3	Catheter Length Analysis	24
3.3.1	Mathematical Model	24
3.3.2	Mathematical Optimization	27
3.3.3	Simulation	28
3.4	Final Detailed Design	28
3.5	Bill of Materials for the Amplifier	32
4	Design Progression	34
4.1	Evolution of Design Solution	34
4.1.1	Major Circuit Revisions from the Previous Prototypes	34
4.2	Technical Challenges and Resolutions	34
4.2.1	MRI System Noise	34
4.2.2	Invasive Blood Pressure Catheter Line Loss	35
4.2.3	Circuitry	35
4.2.4	Shielding	36
4.3	Design Prototype	36

5 Design Testing and Evaluation	38
5.1 Testing Procedures and Results	38
5.1.1 Test I: System Noise Floor Measurement	38
5.1.2 Test II: Clinical Conditions Test	40
5.1.3 Test III: Enclosure Acoustic Testing	41
5.1.4 Test IV: Rigid Cannula Attenuation Testing	42
5.2 Discussion	44
6 Recommendations	45
6.1 Circuit Design Revisions	45
6.2 Human Factors Considerations	45
6.3 Expansion of System Capabilities	46
7 Conclusion	47
8 Project Management	48
8.1 Team Member Roles	48
8.2 Schedule and Intermediate Deadlines	48
Appendix A: User Personas	49
Appendix B: Pressure Attenuation Code	51

List of Figures

1	Image of a fetal heart captured using a gated acquisition. The image on the left shows the ventricles in relaxation, and the image on the right shows the ventricles in contraction. Image credit: Chris Roy - SickKids MRI Lab	2
2	Floor plan of the MRI scan room and control room.	3
3	Previous Transpac IV amplifier prototypes.	6
4	Components of the design solution and their connections.	12
5	Power spectrum of the noise produced by a 3T MRI scanner, measured with an MRI compatible EEG amplifier and an unterminated EEG electrode.	14
6	CMRR vs. Frequency for the LT1167A instrumentation amplifier. Figure courtesy of Linear Technologies.	16
7	RFI input filter schematic.	17
8	Analog devices EMI filter attenuation using standard precision capacitors vs using an X2Y overlapping pair of capacitors.	18
9	LTspice Model Schematic.	20
10	Output of Cable Driver Amplifying Circuit in LTspice.	20
11	Power Supply Rejection Ratio vs. Frequency for the LT1167A Instrumentation Amplifier.	21
12	Infinitesimal transmission line element schematic diagram	25
13	Simulated pressure loss using Equation 19	29
14	Full circuit schematic of the IBP transducer amplifier.	30
15	PCB Layout of the IBP transducer amplifier.	31
16	System noise floor test plan schematic.	39
17	System noise floor testing setup.	39
18	Invasive blood pressure trace recorded on a Yorkshire pig.	40
19	Enclosure acoustic test plan schematic.	42
20	Rigid cannula attenuation test plan schematic.	43

21	Photograph of the line loss testing setup.	43
22	Experimental results of pressure loss with 4m of tubing	44

List of Tables

1	Transpac IV Specifications	14
2	LT1167A Error Budget	15
3	Parameters for skin depth equation	23
4	Parameters for pressure wave equation	27
5	Amplifier Bill of Materials	32
6	Receiver Estimated Bill of Materials	33
7	Project Schedule	48

Acknowledgements

Financial support, test equipment, and project guidance was provided by the members of Chris Macgowan's imaging lab at the Hospital for Sick Children (SickKids). The team would like to thank Chris Roy, Elaine Stirrat, Ruth Weiss, Marvin Estrada, Jun Dazai, Aneta Chmielewski, and Sadie Cook for their assistance with device validation experiments and animal experiment in MRI.

The group would also like to thank Orion Bruckman for his encouragement and proactive assistance throughout the project, and David Wong for sharing his knowledge of fluids modelling.

1

Introduction

1.1 Background on MRI and Gated Acquisition

Clinical magnetic resonance imaging (MRI) scanners have very long acquisition times, typically 30 seconds to 3 minutes per image for 2-dimensional (2D) scans, and 6 to 10 minutes for 3-dimensional scans. This long image acquisition time is problematic for the imaging of dynamic structures such as the heart and coronary arteries, because a standard structural scanning protocol would produce an image that is too blurred for clinical use, because the heart would be moving too much throughout the acquisition. To resolve this problem, researchers reprogram the MRI scanner's sampling and reconstruction software, to use a imaging algorithm called gated acquisition [1].

In a gated acquisition, the motion of the heart is measured and recorded during the MRI scan, typically using electrocardiogram (ECG) or a pulse oximeter. During image reconstruction, the measurements of the heart motion are correlated with the MRI's imaging samples. By correlating the imaging samples with the cardiac phase (heart motion cycle), data from multiple heartbeats can be combined to form a complete image of the heart at the desired point of the cardiac cycle. For example, to measure the heart at diastole (the instant of maximum ventricle relaxation), the MRI scanner would assemble imaging samples from the diastolic phase of hundreds of heartbeats.

Gated acquisition is well established for the cardiac imaging of adults in MRI, and current research at SickKids aims to adapt these techniques for more challenging problems, such as imaging fetal cardiac anatomy, and measuring the blood oxygen saturation of fetuses through image manipulation. The image below is an early result from a clinical trial of a new fetal cardiac imaging protocol. In this acquisition, the MRI scanner was to be gated based on the mother's respiration, and the fetus's cardiac phase. This image is somewhat artifacted, but the fetus's ventricles are clearly

visible.

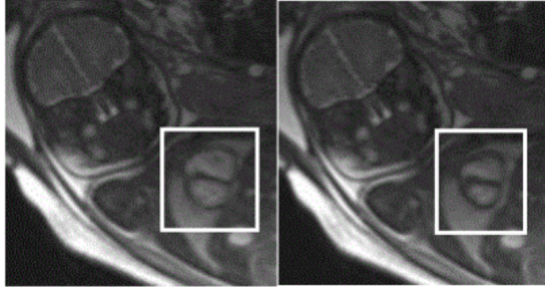


Figure 1: Image of a fetal heart captured using a gated acquisition. The image on the left shows the ventricles in relaxation, and the image on the right shows the ventricles in contraction. Image credit: Chris Roy - SickKids MRI Lab

During the development of gated acquisition scan protocols, researchers frequently test their MRI scan protocols by scanning mechanical models. Various mechanical models are used for different protocols, but most include some type of a pulsatile flow element which mimics the motion of the heart. Also, some advanced gated acquisition protocols, such as those designed for measuring fetal blood oxygen saturation, must be validated on animal models before being used for clinical measurements [2]. During these protocol validation studies, a more precise means of measuring the cardiac phase than the standard non-invasive methods is required [3]. Invasive blood pressure measurement is the method chosen by researchers at SickKids for the next series of protocol validation studies in 2016-2017.

Overview the MRI Environment

The MRI scanner resides inside a custom built room. To protect the operators from accumulative radio frequency radiation exposure, the entire MRI scan room is enclosed in a copper Faraday cage. The only port running between the control room and the scan room is a waveguide, which is 12 centimeters in diameter and located underneath the operator console table. The waveguide is 6 meters away from the MRI scan bed.

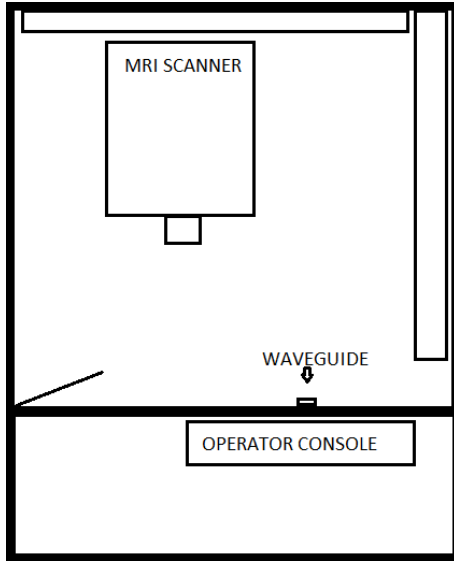


Figure 2: Floor plan of the MRI scan room and control room.

Hazards of the MRI Environment

The SickKids MRI scanner has a base (unchanging) magnetic field strength of 3 Tesla, and a radio frequency output power of 18 kW (roughly comparable to the output power of a local access television transmitter serving a 40 km radius) [4].

The base magnetic field is dangerous, because it will turn any pieces of unsecured ferromagnetic material in the scan room into potentially deadly projectiles. The base magnetic field is always present, even when the scanner is not in use. The high radio frequency output power is also hazardous, because it can induce self heating in conductive materials. In one unfortunate incident in MRI, a pulse oximeter with a poorly designed battery self-heated so severely that it burned a patient's toes off [5]. These objective hazards of the MRI scanning environment mean that all materials placed in the MRI scanner bore must conform to strict engineering standards. For the purposes of animal and mechanical scanning experiments, SickKids performs MRI compatibility testing on all materials in-house, using a 7 Tesla test magnet located in the Toronto Center for Phenogenomics.

There are also several ergonomic safety concerns. MRI technicians and clinical staff need to be able to access the scanner at a moments notice in the case of an

emergency. For this reason, it is essential that all cabling be run on the opposite side the scan room to the door, and that the bed's action is not obstructed by cabling or surgical tubing.

1.2 State of the Art

There are three products on the market for doing invasive blood pressure measurement in MRI. These are: the Transonic ultrasonic blood flow measurement system, the SA instruments invasive blood pressure gating module, and the Samba Preclin IBP measurement module. In 2015, SickKids research institute purchased and tested all three systems, but unfortunately they were all disqualified for use in MRI experiments. The cost of the instruments (the amount paid by SickKids when purchased including accessories), and the reason for disqualification are tabulated below.

Samba Preclin - \$11,500 CAD

This instrument was not fully MRI compatible, because the optical sensor fiber was not long enough to extend from the scanner bed to the control room in Siemens 3 Tesla MRI scanners, forcing the technicians to place the receiver box at the edge of the scan room. The receiver has a ferromagnetic enclosure, so this setup was deemed to be unacceptably dangerous for normal research use. Additionally, the optical catheters cost \$500 each and they were typically destroyed after a single use, making it prohibitively expensive to use this system for dry runs and experiments with mechanical models [6].

Transonic Ultrasonic - \$10,200 CAD

The Transonic flow probe measurement system uses ultrasound to measure blood flow, which can be used as an approximate analog for blood pressure. This system failed to operate correctly while the MRI scanner was running because it was susceptible to the electromagnetic noise emitted by the MRI scanner.

SA Instruments - \$17,000 CAD

This system performed the best of those tested. Unfortunately, this system requires placing a non-MRI compatible module into the scan room, and the system does not provide a means to access the blood pressure measurements outside of the proprietary software included with the device, which was unacceptable for some research applications. This device was also extremely expensive, so SickKids researchers were only able to purchase a single unit to be shared by 25 scientists. This made it difficult to do dry runs and bench top testing with the device before starting animal experiments.

Limitations of Existing Methods

In summary, all of the systems were either dangerous to operate, suffered from interference in the MRI scanner, or were prohibitively expensive. Cost is a major factor in the selection of these devices, because SickKids purchases them using money raised through charitable donation, and there is a strong ethical obligation to minimize research costs wherever possible. Additionally, in the case of the systems with expensive single use probes, it was much more difficult for scientists to do dry runs of animal experiments using mechanical models, which resulted in mistakes being made during those experiments.

1.3 Design Statement

Statement of Need

A low cost invasive blood pressure transducer for use in preclinical MRI studies that maintains the accuracy and cleanliness standards of those already in industry is required. The device must be low cost relative to those already on the market, completely MRI compatible, and be endlessly reusable without needing to replace any expensive components.

Problem Definition

The problem addressed by this design project is that medical researchers at SickKids require an MRI compatible invasive blood pressure measurement system for use in experiments using mechanical and animal models, but there are no suitable products on the market.

1.4 Previous Work

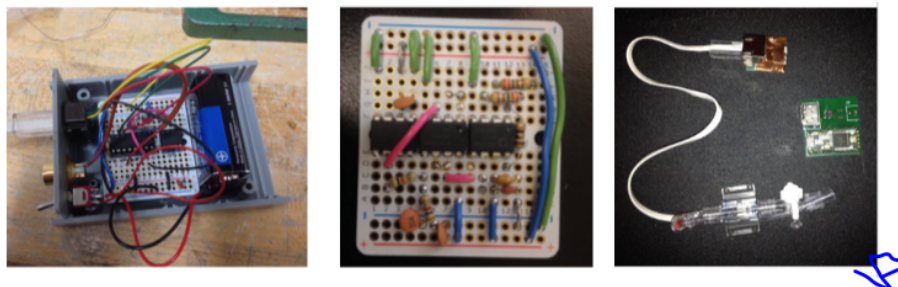


Figure 3: Previous Transpac IV amplifier prototypes.

Previous amplifier prototypes built by Josh Bradshaw in early 2015 used low voltage, single supply components and relied on digital filtering methods to attenuate the MRI system noise to an acceptable level. This approach was not effective, because the amplifier was frequently pushed into saturation by electrical interference when the MRI scanner was operating in its high power mode.

1.5 Project Goals and Objectives

To measure invasive blood pressure in real time, several components are required. Those components include:

1. An invasive blood pressure transducer, with all associated surgical supplies. For this project the Transpac IV transducer, by ICU medical was used.
2. An MRI compatible measurement instrument connected to the sensor to precisely amplify and measure the blood pressure signal.

3. A communications system to transmit the blood pressure measurements from the scanner bed to any relevant MRI gating systems and patient monitoring systems in real time.

The design focus of this project was building the measurement instrument and communications system. The suitability and accuracy of the Transpac IV transducer, surgical protocol for catheter insertion, and MRI imaging protocols have all been established by researchers at ICU medical and SickKids respectively, therefore there was no further study of these areas during this project.

1.6 Expected Impact

MRI compatible invasive blood pressure measurement instruments are exceptionally expensive. Any cost savings would help expedite research by reducing financial burdens.

This device is anticipated to cost \$300 – \$500 and be endlessly reusable. This will expedite preclinical research by making it easy and affordable for new labs to get involved in replicating studies that require IBP measurement capabilities. Finally, the design will be open source and released in an MRI instrumentation journal, the reference design will help other researchers around the world to design their own MRI compatible measurement instruments. The same components used to build this system could be used for the development of low cost squeeze bulb interfaces for fMRI studies or balloon type respiration monitors.

2

Requirements and Specifications

2.1 Design Requirements

Medical Device Sterility Requirements

When animals are present in the MRI scanner, the scan room is subject to the same regulations as any other room of the hospital in which minor surgeries take place . This means that the device must be simple to disassemble and clean.

SickKids uses a variety of techniques to clean medical equipment. The practices relevant to this design are:

1. Hard (non-porous) surfaces not in direct contact with bodily fluids such as IV poles, the MRI scanner, and patient monitors are typically cleaned using chemical solutions.
2. Instruments in direct contact with patients bodily fluids must either be autoclaved or disposed of.
3. No adhesives may be used in the MRI scan room, because glue residue stuck on surfaces renders chemical treatments ineffective [7].

These standards severely limit the materials available. To ensure a low device cost, it is essential to ensure the hospital's disease control staff is able to clean the device effectively without damaging it or disposing of expensive components every time that it is used.

Functional Requirements

For general research use at SickKids, the system must have a measurement accuracy of ± 2 mmHg, without requiring any manual calibration beyond zeroing the monitors just before connecting the invasive blood pressure line to the arterial catheter.

Additionally, the measurement must be available in real-time to the veterinary staff, who may use the measurement to make decisions about animal care.

User Requirements

Given that this is a tool for scientific research, the system has two primary personas: veterinary staff and MRI researchers. A description of these users, their desires, and their goals for the device can be found in Appendix A.

The veterinary staff's requirements are:

1. The system must be easy to assemble and calibrate in the operating room.
2. The pressure probes must be implantable using conventional surgical technique.
3. The system must provide a means for mechanically stabilizing the invasive pressure catheters.
4. The system must be easy to disassemble and clean at the end of the experiment.
5. The system must provide them with the animal's systolic and diastolic pressures in real time, for physiological monitoring purposes.

The user requirements of the MRI researchers are:

1. The system must not interfere with the regular operation of the MRI scanner by introducing image artifact or impeding the motion of the scanner bed.
2. The cabling and apparatus must be minimally obtrusive, so that the technicians can respond to any equipment emergencies immediately.

Engineering Requirements

Based on the functional and user requirements, the following engineering requirements were developed.

1. Pressure measurement should be accurate to the industry standard specification of ± 2 mmHg.

2. Measurement instrument should be able to withstand at least 100 operating room cleaning cycles.
3. Capable of measuring pressures over the full linear range of the transducer (0 – 200 mmHg)

Mechanical Constraints

The system is subject to two major mechanical constraints. The first is that there is only one small hole in the wall between the MRI scan room and the control room to accommodate cabling, and this port is specially designed to prevent any RF radiation from leaking through into the control room. This means that all forms of wireless communication between the scan room and the control room are impossible. It also means that the amount of cabling running to the device must be minimized, because the cable has to pass through a long waveguide, then across the entire scan room, where it could present a tripping hazard.

The second mechanical constraint is that the MRI scanner bed is repeatedly inserted and removed from the MRI scanner bore throughout the experiment to allow the veterinary staff to administer medications, adjust the ventilator pressures, and check on the animal. This means that the system must have long enough cabling to accommodate this change in position, and provide sufficient mechanical stabilization for the invasive blood pressure line and IV line to ensure that they can't be tugged during insertion or removal. If either line is tugged out of place, death of the animal subject is inevitable.

MRI Compatibility Requirements

The MRI compatibility standard dictates that the major hazards of the MRI environment, in order of precedence, are:

1. The risk of ferromagnetic objects being propelled across the scan room in an uncontrolled manner by the scanner's magnetic field.

2. The risk of materials self-heating to dangerous temperatures when exposed to the scanner's high power RF radiation.
3. The risk of paramagnetic materials producing distortions on the MRI scanner's imagery.

To ensure that the device is entirely MRI compatible, none of the components placed in the MRI scan room can be ferromagnetic or paramagnetic. Additionally, to avoid any self-heating the device must minimize inductive loops in the circuitry. Finally, to eliminate the risks of image distortion, no electrically conductive material can be placed in the MRI scanner's bore.

2.2 Overview of Design Solution

The major components of the system are:

1. The blood pressure transducer, the Transpac IV, which is MRI compatible [12] [13].
2. The amplifier circuitry.
3. The shielding and cabling system.
4. The power supply and signal receiver.

The connections between the components are illustrated in the map diagram below:

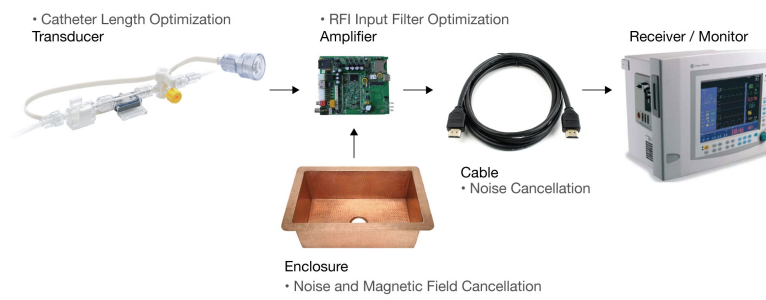


Figure 4: Components of the design solution and their connections.

3

Engineering Analysis

3.1 Circuit Design Overview

The circuitry is divided into the following sections:

1. An off-the-shelf Transpac IV blood pressure transducer, using a modified Wheatstone bridge topology.
2. EMI input filter.
3. Instrumentation amplifier.
4. Cable driver.
5. Power supply filter.

Electromagnetic Interference Analysis

The MRI scanner emits high frequency noise with a maximum output power of 18 kW. This high frequency noise can couple into the measurement system through parasitic inductance and capacitance in the circuitry, producing measurement errors. This type of interference caused the failure of the Transonic measurement unit and the two previous prototypes of this measurement unit.

The noise produced by the MRI scanner has a 27 MHz base-band frequency and a 200–300 Hz modulation frequency [8]. The variations in the modulation frequency are illustrated in the spectral plot below, which was recorded by an MRI instrumentation research group.

The type of noise emitted by MRI scanners is particularly problematic, because the scanner continuously varies its output power and modulation frequency throughout the scan, making it difficult to troubleshoot measurement errors.

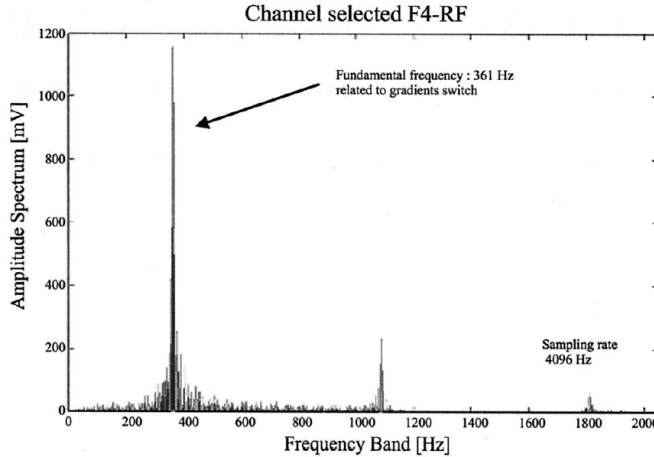


Fig. 2. Main dominant frequencies carry out from gradient switching events.

Figure 5: Power spectrum of the noise produced by a 3T MRI scanner, measured with an MRI compatible EEG amplifier and an unterminated EEG electrode.

Transpac IV Analysis

The Transpac IV measures gauge pressure using a bridge type strain gauge element. The relevant specifications for the Transpac IV are given below:

Table 1: Transpac IV Specifications

Pressure Range	0 – 300 mmHg
Supply Voltage	0 – 10 V_{dc} (specified at 6V)
Zero Pressure Offset	-0.75 – 0.75 mV
Sensitivity	5.0 μ V/V/mmHg
Span at 100mmHg	3.006 mV
Linearity	$\pm 1.5\% V_{FSS}$
Accuracy from 0-200mmHg	$\pm 1.5\%$
Stability	$\pm 0.5\% V_{FSS} \Omega$
Input Impedance	4500 Ω
Output Impedance	300 Ω

The worst case error due to zero pressure offset while driving the bridge with 6 V_{DC} is:

$$\text{Offset Error} = \frac{\pm 0.75mV}{5.0 \frac{V}{mmHg} * 6V_{DC}} = \pm 25mmHg$$

The zero pressure offset means that the measurement recording system must always be zeroed before making measurements, or else the system will exhibit offset errors of up to $\pm 25 mmHg$.

Considering the transducer's worst case linearity and accuracy specifications, the expected accuracy in practical use measuring pressures of $60 - 140 mmHg$ is $\pm 2 mmHg$, which is an industry standard specification for invasive blood pressure transducers.

Amplifier Selection

The LT1167A amplifier was chosen, based primarily on its inclusion in a reference design of a similar system [9]. The error budget for this amplifier is given below [10]:

Table 2: LT1167A Error Budget

Offset voltage	40 V
Noise Voltage	0.28 uVpp typical
Power Supply Rejection	0.28 Vpp/100mV change
CMRR	105dB minimum
PSRR	105dB minimum
Input Offset Current	0.11uV/350Ω

This amplifier is ideal for use in MRI, because it has best in class common mode and power supply rejection ratios, which help to minimize the effects of MRI scanner noise. Additionally the LT1167A has an exceptionally low input bias current of 350 pA max, ensuring that the parasitic voltage across the bridge will be negligible.

EMI Input Filter Design

The purpose of the first filter stage is to attenuate the 27MHz base-band frequency. The output of an ideal differential amplifier is:

$$V_o = A_d(V_+ - V_-) + \frac{1}{2}A_{cm}((V_+ - V_-))$$

Where A_d is the differential gain and A_{cm} is the common mode gain. In an ideal differential amplifier $A_{cm} = 0$. In practice all amplifiers exhibit some common mode gain and amplifier manufacturers specify their products based on their common mode rejection ratio (CMRR):

$$CMRR = \frac{A_d}{|A_{cm}|}$$

The common mode rejection ratio of the amplifier is frequency dependent. The CMRR plot for our chosen instrumentation amplifier is given below:

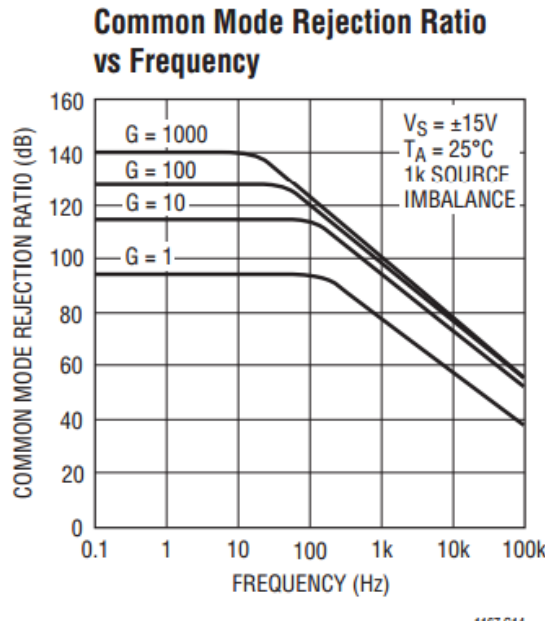


Figure 6: CMRR vs. Frequency for the LT1167A instrumentation amplifier. Figure courtesy of Linear Technologies.

As shown in the plot, the LT1167A has an excellent CMRR within its 120 kHz bandwidth, but outside the amplifier's bandwidth, the CMRR quickly approaches 0 dB. This means that any common mode radio frequency signal at the amplifier's inputs will be rectified by the amplifier, producing intermittent DC offset errors.

To overcome this instrumentation amplifier limitation, it was necessary to place a low-pass filter between the Transpac IV transducer and the amplifier. The basic filter design taken from a reference design by Analog Devices [11].

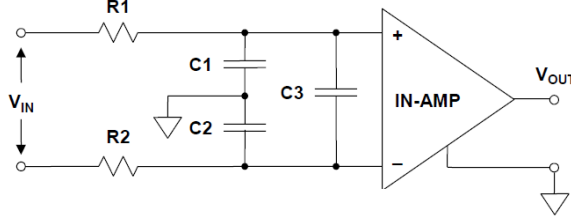


Figure 7: RFI input filter schematic.

The bandwidth of the invasive blood pressure signal is DC-15 Hz, so based on the recommendations of the application note, the acceptable range of cutoff frequencies was 1 kHz - 5 kHz to ensure that the filter did not exhibit any pass-band distortion in the DC-15 Hz bandwidth.

The differential cutoff frequency of this circuit is:

$$\tau_{DIFF} = (R_1 + R_2) \left[\frac{C_1 C_2}{C_1 + C_2} + C_3 \right]$$

The common mode cutoff frequency of this circuit is given by:

$$\tau_{CM} = R_1 * C_1$$

Assuming that:

$$\tau_{CM} = (R_1 C_1) = R_2 C_2$$

$$R_1 = R_2$$

$$C_1 = C_2$$

$$BW_{DIFF} = \frac{1}{2\pi(R_1 + R_2)[\frac{C_1 C_2}{C_1 + C_2} + C_3]}$$

For this circuit to function correctly the ratio-metric equality $R_1/C_1 = R_2/C_2$ must be accurate to within 1%, because if this ratio is unbalanced, common mode

noise will be converted into differential noise. This restriction made component selection challenging, because low-cost 1% matched pairs of capacitors are only available in a limited range of values.

The output impedance of the Transpac IV sensor is approximately 300Ω , with variations with pressure from $290 - 310 \Omega$ in the pressure range of interest. To ensure that variations in the Transpac's IV's output impedance have negligible effect on the ratiometric equality of the filter sections $R_1 = R_2 = 4.02 k\Omega$ was chosen. Placing resistors of two orders of magnitude greater than the maximum change in bridge output impedance ensures that in the worst case, the differential bridge impedance will only produce a 0.5% ratio error [12].

To achieve a differential cutoff frequency in the desired range of $1 kHz - 5 kHz$ while using this high resistor value, $C_1 = C_2 = 10 nF$ was chosen, resulting in a differential cutoff frequency of 4 kHz. The capacitor pair chosen was a 0.05% matched pair of X2Y capacitors (X2Y is a relatively new type of capacitor, in which two matched capacitors are placed on a single die), and C_3 was omitted because the X2Y matched pair provided sufficient common mode attenuation to make it redundant, as illustrated in the plot below [14].

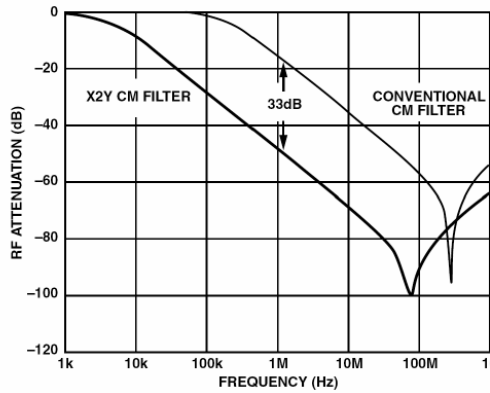


Figure 6: RF Attenuation for X2Y vs. Conventional RC Common-Mode Filter

Figure 8: Analog devices EMI filter attenuation using standard precision capacitors vs using an X2Y overlapping pair of capacitors.

Cable Driver Amplifier

An HDMI cable has a maximum capacitance of 27 pF/m , and depending on the particular MRI scanner, a cable of up to 10m in length is required to reach the bore of the magnet [15]. Most operational amplifiers can not drive capacitive loads, because the capacitive load on the output adds an additional pole to the feedback loop, increasing amplifier overshoot and decreasing the amplifier's stability margin.

The primary criterion for the cable driver amplifier was that it had to be specified for driving a large capacitive load. Additionally, the amplifier had to be unity gain stable, with good DC performance. Based on these considerations, the LT1357 was chosen for the cable driver amplifier.

Simulation

To ensure that the cable driver amplifier would not exhibit oscillations while driving the HDMI cable, the cable driver amplifier was simulated by running a sine function with a DC offset of -3 V and an amplitude of 1 V at 300 Hz through the cable driver amplifier circuit in LTspice, with the amplifier outputs connected to a worst case cable impedance. The results were examined to see if any significant transients or oscillations arose from either of the two LT1357 amplifiers used in the circuit. The results showed no transients, seen in Figure 10.

Power Supply Filter

Similarly to the common-mode rejection ratio, the amplifier's power supply rejection ratio also degrades to negligible levels at high frequencies. Thus, a filter must be placed at each power pin of the amplifier circuitry to attenuate the high frequency noise, which would otherwise cause intermittent DC offset errors at the output.

Based on an application note on amplifier decoupling in environments with high power electromagnetic noise, a power supply filter consisting of three bypass capacitors of values 100 μF , 0.33 μF and 0.1 μF was placed on every power pin of every amplifier [16].

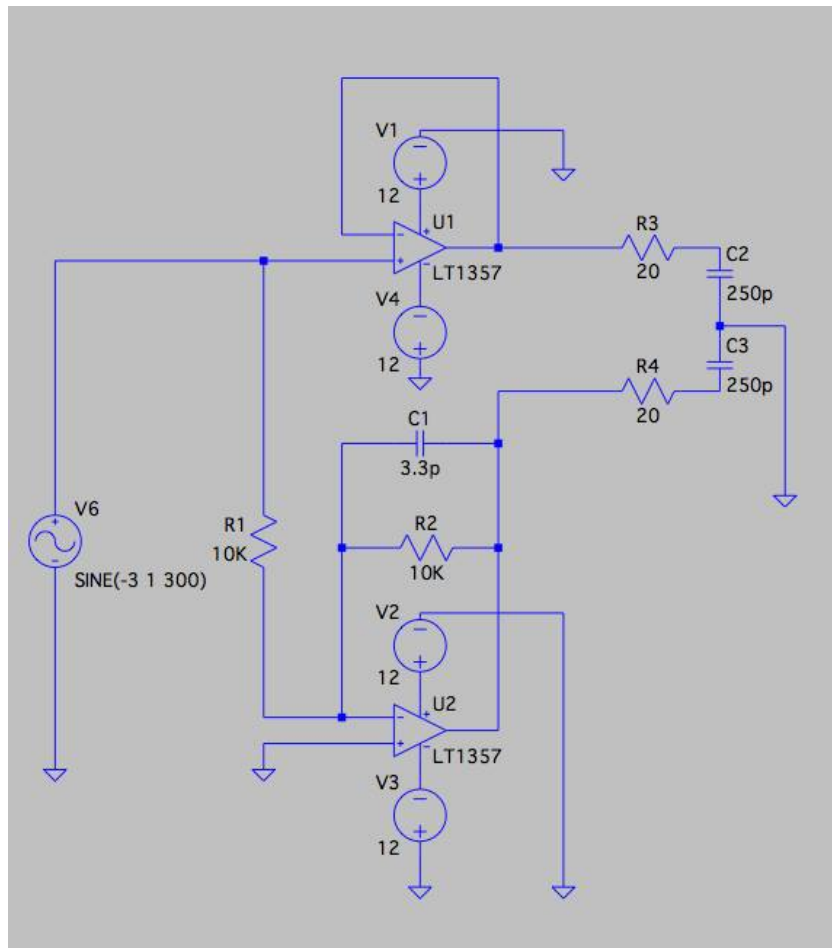


Figure 9: LTspice Model Schematic.

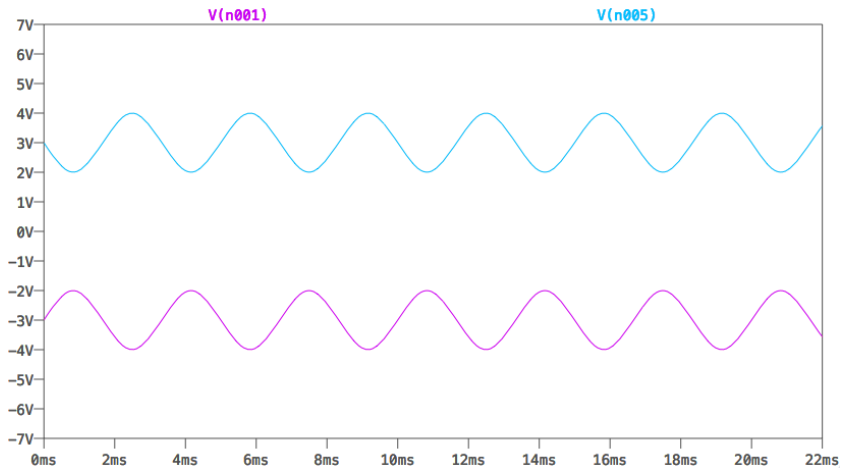


Figure 10: Output of Cable Driver Amplifying Circuit in LTspice.

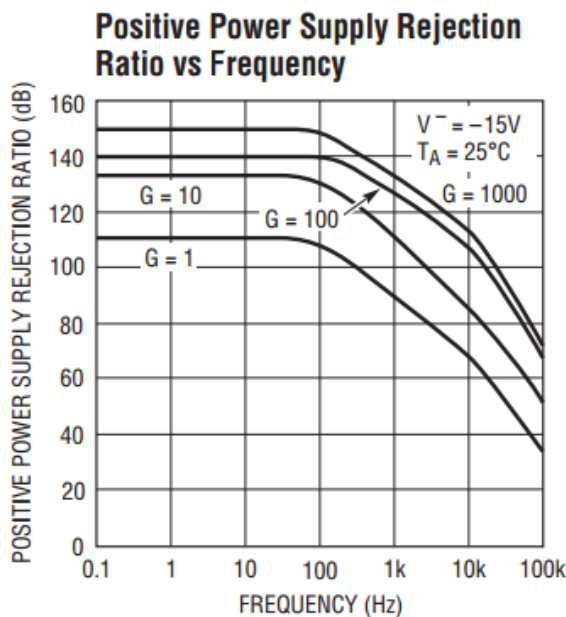


Figure 11: Power Supply Rejection Ratio vs. Frequency for the LT1167A Instrumentation Amplifier.

Cable Selection

In this design, we required a shielded, MRI compatible cable with at least five conductors. As of time of writing, SickKids policy dictates that only two types of cabling are unconditionally approved for use in their MRI scanners: Belden coaxial cable and MRI compatible HDMI cabling. For this design, HDMI cabling was chosen, because of the conveniently small connector footprint and the positive experiences that other SickKids design engineers had while using it in thermocouple amplifier designs.

Bridge Driver

To drive the bridge, a TPS709 LDO manufactured by Texas Instruments was selected. This LDO was chosen because it has 0.2% line regulation, which is sufficiently accurate for the application, and it is capable of driving a short circuit indefinitely, which ensures that the LDO will not be destroyed in the event of transducer failure.

PCB Design for MRI Compatibility

The PCB was designed to minimize the capacitive and inductive coupling with the MRI scanner, and to ensure that the amplifiers functioned as well as possible. The PCB layout was designed by hand, by first laying out each amplifier section outside of the board area, in accordance with the component manufacturer's layout recommendations. Next, these sections were dragged into the board area and arranged in such a manner that signal trace lengths were minimized. Power planes and continuous ground planes were used to minimize trace impedance, which was an especially important consideration around the analog input filter.

Altium circuit maker's design rule check was used to find and eliminate all single ended and dead copper, which would otherwise act like antennas. Finally, a patch of solder resist was left off at each end of the circuit board, so that the shield could make a low impedance connection to the ground plane.

3.2 Shielding Analysis and Design

An enclosure than can protect the pressure transducer and the transducer amplifier from high power electrical and magnetic noise noise present in the MRI scanning environment is important to ensure proper function of the system.

Mathematical Model

Shielding against low frequency magnetic fields, such as the noise due to gradient switching, is typically done using thick sheets of magnetically permeable material, such as mu-metal. The mu-metal's high magnetic susceptibility allows the enclosure to absorb the magnetic field's energy and minimize the magnetic field's effect on the internal circuitry. However, materials with a high magnetic susceptibility are not MRI compatible so shielding against low frequency magnetic noise is not possible in this application. However, shielding against the high frequency, short wavelength noise was feasible. Any fully enclosed Faraday cage with a sufficiently thick skin depth effective at attenuating radio frequency noise [17].

The equation for skin depth is [18]:

$$\delta = \sqrt{\frac{\rho}{\pi f \mu}} \quad (1)$$

Material Selection

It was essential that the shielding material have negligible ferromagnetic and paramagnetic susceptibilities. Copper was chosen, because it has negligible ferromagnetic and paramagnetism susceptibilities (hence its use in MRI superconductors) and it is the only material shielding material that is approved for use within the MRI scanner's bore [19]. The only alternative material, aluminum, was eliminated from consideration because most aluminum alloys have greater paramagnetic susceptibility than copper, and pure aluminum foil was more expensive than copper foil.

Minimum Shield Thickness Calculation

To ensure that the shield will entirely block the MRI scanner's base-band noise, it must have a sufficiently thickness to carry the radio frequency current.

The skin depth Equation 1 and the values specified for the material properties of copper are given in Table 3.

Table 3: Parameters for skin depth equation

Symbol	Variable	Value	Units
δ	skin depth		m
ρ	resistivity	1.68×10^{-8}	Ωm
f	frequency of noise	127×10^6	Hz
μ	permeability	$4\pi \times 10^{-7}$	$\frac{H}{m}$

Substituting these values into Equation 2 yielded a minimum skin depth of:

$$\delta = 5.857 \mu m \quad (2)$$

It is concluded that a shield thickness greater than $5.857\mu m$ will be effective at blocking MRI scanner's base-band frequency noise. For the prototype's shield, copper foil tape with a conductive adhesive was used. The thinnest tape available had a thickness of $66\mu m$, which is approximately 11 times greater than minimum thickness required for this application. This tape was used to shield the amplifier by wrapping it tightly around the entire circuit board, creating a Faraday cage. Copper tape is very expensive (\$30 per square foot), so in a production version of this device, a copper plated enclosure would be used instead.

3.3 Catheter Length Analysis

The MR environment produces a large amount of electrical noise and the power of this noise decreases cubically in proportion to the distance from the MRI. Therefore, the length of tubing that runs between the patient and the transducer governs how much noise the the transducer and amplifier system are subject to. However, increasing the length of the tubing runs the risk of causing pressure signal attenuation before it reaches the pressure transducer. The goal of this optimization is to determine the maximum length of the catheter tubing that can be used without major signal attenuation of ($< 1 \text{ mmHg}$ or 133 Pa pressure loss).

Mathematical Model

Pressure wave losses in a static fluid are commonly modelled using Transmission Line Theory, which is the modelling approach chosen for this analysis. Figure 12 shows the circuit model for an infinitesimal length of a uniform transmission line [20]. The signal variables V for potential and I for flow are general. With appropriate assumptions this model can apply to electrical, fluid, or other continuous media.

Pressure Wave Equation Derivation

Applying Kirchoff's Voltage and Current laws to the circuit in Figure 12 gives:

$$V_{in} - V_{out} - V\dot{R} - V\dot{L} = 0 \quad (3)$$

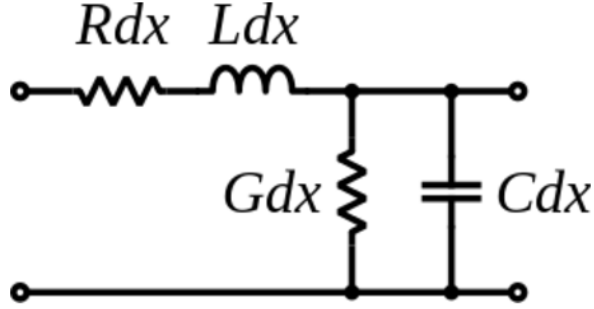


Figure 12: Infinitesimal transmission line element schematic diagram

$$I_{in} - I_{out} - I\dot{C} - I\dot{G} = 0 \quad (4)$$

By dividing these equations by Δx and taking $\lim \Delta x \rightarrow 0$ gives the following second order differential equations:

$$-\frac{\partial i(x, t)}{\partial x} = \dot{G}v(x, t) + \dot{C}\frac{\partial v(x, t)}{\partial t} \quad (5)$$

$$-\frac{\partial v(x, t)}{\partial x} = \dot{R}i(x, t) + \dot{L}\frac{\partial i(x, t)}{\partial t} \quad (6)$$

Converting Equations 5 and 6 into phasor form gives:

$$-\frac{d\tilde{I}(x)}{dx} = (\dot{G} + j\omega\dot{C})\tilde{I}(x) \quad (7)$$

$$-\frac{d\tilde{V}(x)}{dx} = (\dot{R} + j\omega\dot{L})\tilde{V}(x) \quad (8)$$

Combining Equations 7 and 8 results in the second order differential wave equation in phasor form:

$$\frac{d^2\tilde{V}(x)}{dx^2} - \gamma^2\tilde{V}(x) = 0 \quad (9)$$

Where γ is:

$$\gamma^2 = (\dot{R} + j\omega\dot{L})(\dot{G} + j\omega\dot{C}) \quad (10)$$

$$\gamma = \alpha + j\beta \quad (11)$$

where

$$\alpha = Re(\gamma) = Re(\sqrt{(\dot{R} + j\omega\dot{L})(\dot{G} + j\omega\dot{C})}) \quad (12)$$

$$\beta = Im(\gamma) = Im(\sqrt{(\dot{R} + j\omega\dot{L})(\dot{G} + j\omega\dot{C})}) \quad (13)$$

The various elements in this circuit as they are defined using fluid properties are:

- Resistance:

$$R = \frac{V}{I} = \frac{\Delta P}{Q} = \frac{32\mu x}{Ad^2} \quad (14)$$

- Conductance:

$$G = \frac{1}{R} = \frac{Q}{\Delta P} = \frac{Ad^2}{32\mu x} \quad (15)$$

- Capacitance:

$$C = \frac{I}{\dot{V}} = \frac{Q}{\Delta P} = \frac{V}{\beta} + \frac{A^2}{k} = \frac{Ax}{\beta} + \frac{A^2}{k} \quad (16)$$

- Inductance:

$$L = \frac{V}{\dot{I}} = \frac{\Delta P}{\dot{Q}} = \frac{\rho x}{A} \quad (17)$$

Solving equation 9 and converting it back into the time domain gives the equation for pressure, a partial standing wave:

$$p(x, t) = |P_o^+|e^{-\alpha z} \cos(\omega t - \beta z + \phi^+) + |P_o^-|e^{\alpha z} \cos(\omega t + \beta z + \phi^+) \quad (18)$$

Where ϕ , P_o^+ and P_o^- are from the initial conditions of the system. The parameters for the system are in Table 4. Because the parameter values for 0.9% saline are not tabulated, the system was modeled using the parameters for water.

Table 4: Parameters for pressure wave equation

Symbol	Variable	Value	Units
μ	dynamic viscosity	1.002×10^{-3}	$\frac{Ns}{m^2}$
x	length of tubing	variable	m
A	cross-sectional area of tubing	2.4×10^{-6}	m^2
d	diameter of tubing	1.9×10^{-3}	m
V	volume of tubing	xA	m^3
β	bulk modulus of fluid	2.19×10^9	$Pa, \frac{N}{m^2}$
k	compressibility of container	negligible	$\frac{1}{Pa}, \frac{m^2}{N}$
ρ	density of fluid	988.2	$\frac{kg}{m^3}$
P_o^+, P_o^-	pressure coefficient	assumed to be 16000	Pa
φ	initial wave phase	assumed to be 0	$^\circ$

Mathematical Optimization

Objective Function

The most important characteristic of the wave for the purposes of modelling the signal attenuation. Therefore, the objective function will be a modified version of Equation 18, which models the upper bound of the forward propagating wave:

$$p(x, t) = |P_o^+| e^{-\alpha z} \quad (19)$$

This equation represents the upper bound of the blood pressure wave.

Design Parameters Optimized

The length of the tubing x was maximized while spatial decay α was minimized. Maximizing the length of the tubing reduced the amount of electrical noise the amplifier circuitry is subject to while Minimizing the spatial decay reduces the pressure wave signal attenuation before it reaches the circuitry.

Constraint Equations

The length of the catheter tubing must be greater than or equal to zero.

$$x \geq 0 \quad (20)$$

Dynamic viscosity μ , cross-sectional area of the tubing A , diameter of the tubing d , bulk modulus of the fluid β and the density of the fluid ρ are all restricted to the known values for the fluid. These values for water are listed earlier in Table 4.

The cross-sectional area A , diameter d , and compressibility k of the tubing are restricted to by the tubing size available for use with the Transpac IV. These values are also listed earlier in Table 4.

Starting Values of Design Parameters

The length of the tubing will be varied starting from 0 to 150 meters in 0.1 m increments. All other values are fixed as listed in Table 4.

Simulation

Simulating the upper bound of the pressure loss from Equation 19 resulted in the plot in Figure 13. The code for this simulation is available in Appendix B.

The results of the simulation indicated that the signal experiences:

- 1200 Pa or 9 $mmHg$ of pressure loss with 150 m of tubing
- 200 Pa or 1.5 $mmHg$ of pressure loss with 50 m of tubing
- 0 Pa of pressure loss with 4 m of tubing

Based on these results, the pressure losses associated with increasing the tubing length up to 50 meters will produce negligible losses. Testing to confirm this simulation are discussed in Section 5.1.4.

3.4 Final Detailed Design

Drawings and estimated bill of materials for a fully commercialized system are presented below. This system will never be produced in volume, so the 10X quantity

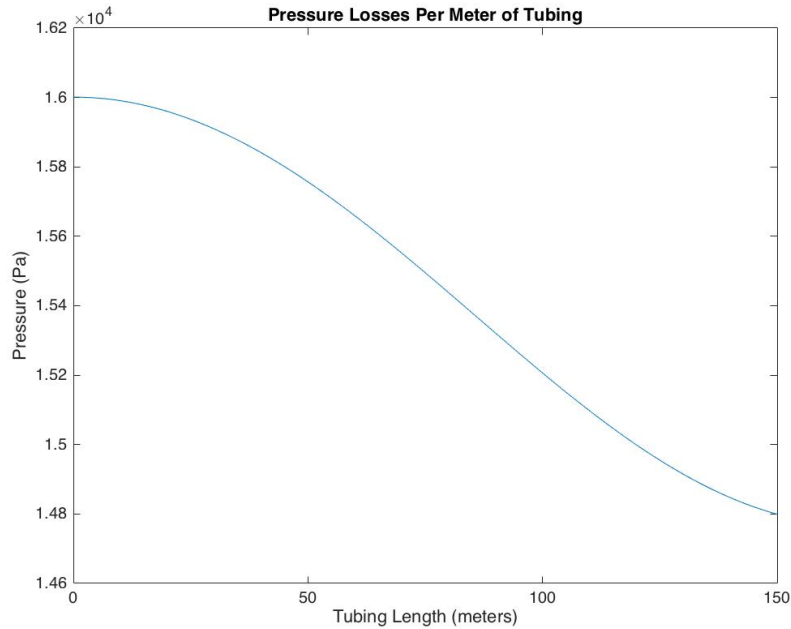
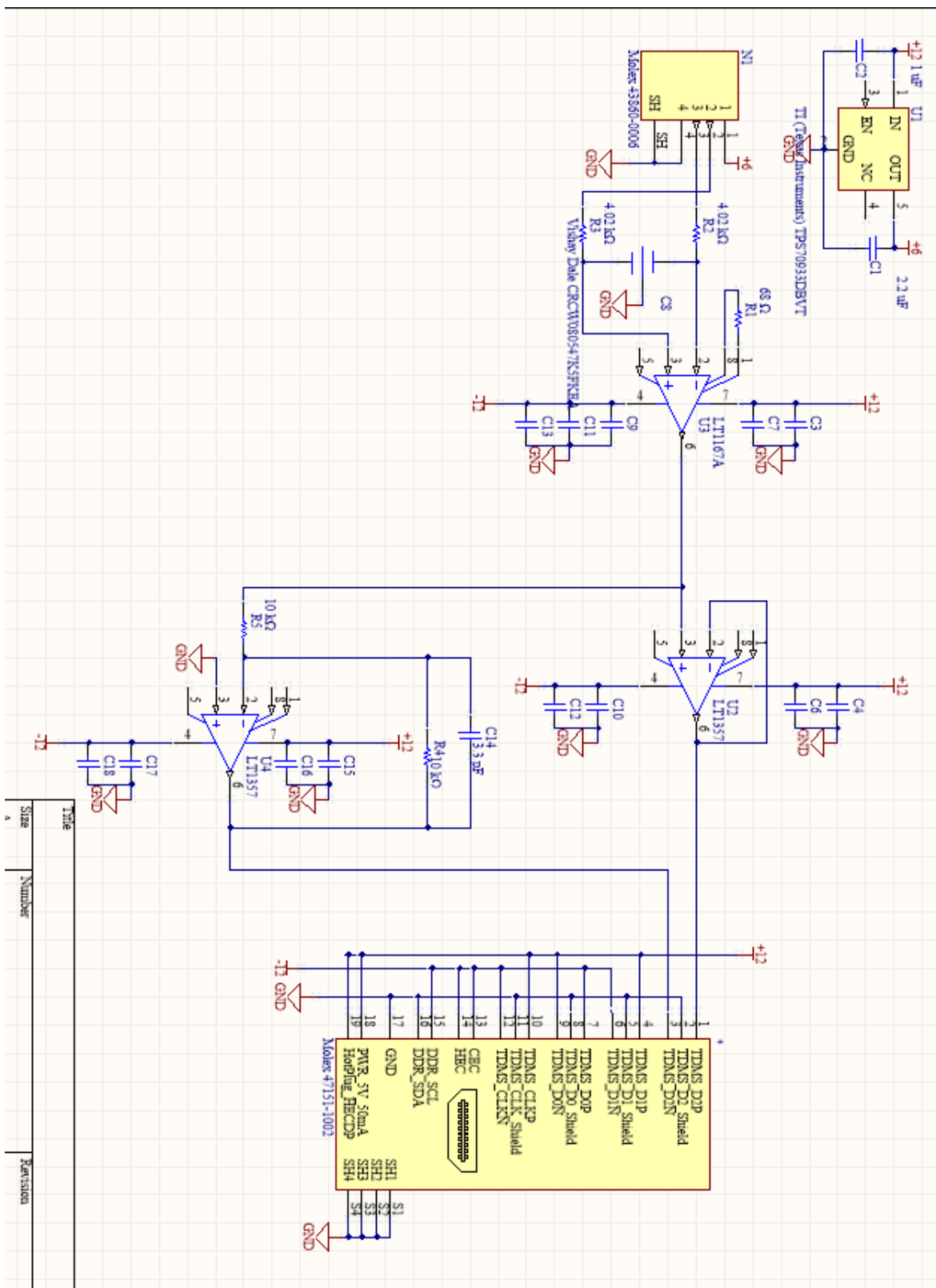


Figure 13: Simulated pressure loss using Equation 19

prices are used throughout. The receiver module is not yet fully designed, so rough estimates have been provided in its bill of materials. The receiver schematic and PCB layouts have not been completed as of time of writing, because they fall outside the intended scope of this design project. They will be finished in late April, before the next prototype of this system goes into production.

The circuit schematic for the IBP amplifier is given below.



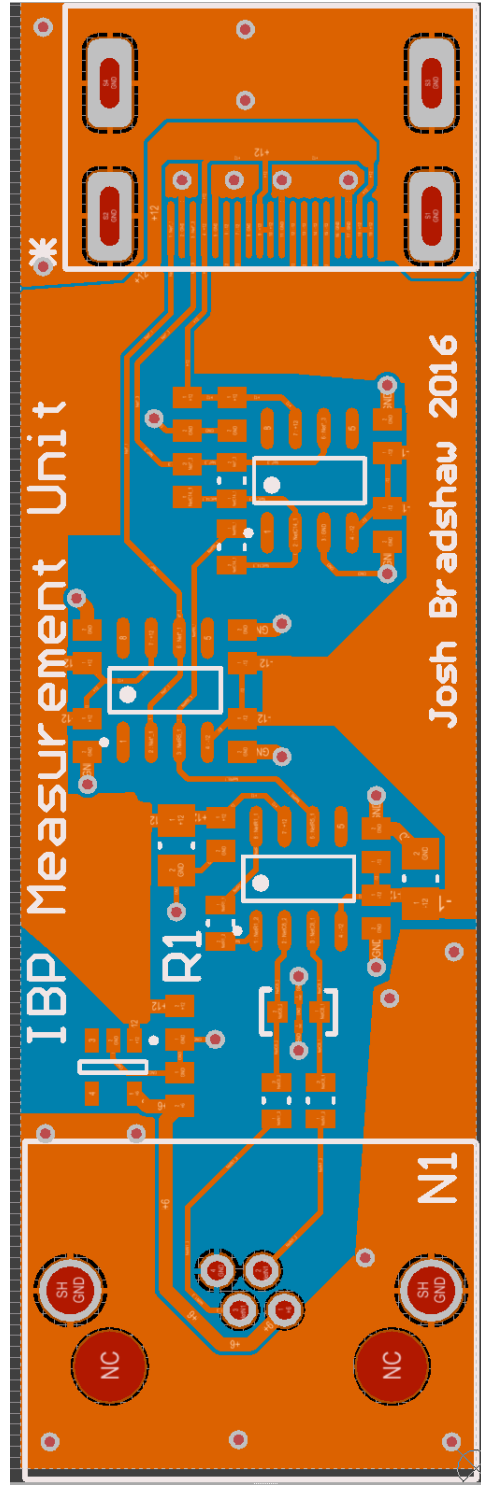


Figure 15: PCB Layout of the IBP transducer amplifier.

3.5 Bill of Materials for the Amplifier

Table 5: Amplifier Bill of Materials

Component	Quantity	Unit Price at 10x Quantity (\$)
LT1167A	1	10.5
LT1357	2	8.5
PCB	1	10
EMI FILTER 10NF 100V X2Y 0805	1	1.82
IC REG LDO 6V 0.15A SOT23-5	1	1.78
CONN MOD JACK 6P4C R/A SHIELDED	1	2.82
CAP CER 0.33UF 50V Y5V 0805	7	0.005
CAP CER 0.1UF 50V Y5V 0805	7	0.005
CAP CER 10000PF 50V X7R 0805	7	0.03
RES SMD 10K OHM 0.1% 1/8W 0805	2	1
CAP CER 3.3PF 50V NP0 0805	7	0.037
CONN RCPT 19POS HDMI RT ANG SMD	1	3.84
CAP CER 47UF 25V X5R 1206	7	1.53
CAP CER 2.2UF 50V X5R 0805	7	0.71
CAP CER 1UF 50V X7R 0805	7	0.31
RES SMD 68 OHM 0.1% 1/8W 0805	7	0.84
RES SMD 4.02K OHM 1% 1/8W 0805	3	0.033

Table 6: Receiver Estimated Bill of Materials

Component	Quantity	Unit Price at 10x Quantity (\$)
Analog to digital converter	1	11.5
Teensy 3.1 uC	1	12
PCB	1	10
Various passive components	10-20	0.005
USB Cable	1	3
Power Supply	1	30-150

4

Design Progression

4.1 Evolution of Design Solution

The final design solution remained similar in concept to the initial design concept. However, a number of significant revisions to the components were completed as more research was completed. These changes will be discussed below.

Major Circuit Revisions from the Previous Prototypes

Previous prototypes, pictured in Figure 3 for the system are discussed in Section 1.4. These prototypes did not achieve the accuracy goal of ± 2 mmHg, so several changes were made in this revision in an attempt to improve the system's signal to noise ratio.

4.2 Technical Challenges and Resolutions

MRI System Noise

Previous amplifier prototypes built by Josh Bradshaw in early 2015 used low voltage, single supply components and relied on digital filtering methods to attenuate the MRI system noise to an acceptable level. These prototypes did not achieve the accuracy goal of ± 2 mmHg, so several changes were made in this revision in an attempt to improve the system's signal to noise ratio.

The first and most important change is that the supply voltage was increased from a 3.3 V single supply to a ± 15 V split supply. Increasing the supply voltage range by an order of magnitude substantially reduces the system's susceptibility to noise. Another important change is that in this revision, an EMI filter was added between the Transpac IV transducer and the first gain stage to prevent RF noise from the MRI scanner from being rectified by the amplifier. Finally, the output was changed from being a single-ended ground referenced signal to a differential pair, ensuring that any

currents flowing through the shielding do not contribute to measurement errors.

Invasive Blood Pressure Catheter Line Loss

Before commencing this design project, it was unknown whether a 2 m invasive blood pressure arterial line could be used without introducing significant measurement error by attenuation. This was problematic, because an arterial line of at least 2 m long was required to accommodate the insertion and removal of the MRI scanner bed from the bore. This problem was resolved by creating an acoustic model of the arterial line and performing acoustic testing with various lengths of tubing. The conclusion from the testing and modelling was that the line pressure losses will be negligible for the tubing length and frequency ranges used in this system.

Determining the best model for this system proved to be quite difficult. A survey of a number of research articles involving wave modelling in static fluid was conducted. The system could have possibly been modeled as a water hammer, but this assumes that the fluid in the piping is initially moving, then the flow is suddenly stopped, which does not accurately represent the IBP system [21].

After a lack of results from the literature survey, David Wong, a graduate student at the University of Waterloo studying microfluidics was contacted to provide advice on the best method of modelling the catheter system. After an initial meeting in which the method of modelling the system using Transmission Line Theory [20] was discussed, he provided some guidance in the derivation process as it applies to static fluid systems. From there is was possible to model the blood pressure wave using Transmission Line Theory.

Circuitry

The principle technical challenges of designing the amplifier circuitry were adhering to MRI compatibility standards and preventing the high power RF noise produced by the MRI scanner from corrupting the measurement.

Adhering to MRI compatibility limited component selection considerably. The vast majority of batteries, EMI filters, cable connectors, and shielded enclosures are

not MRI compatible. Typical EMI filters include electrolytic capacitors and ferrite beads, neither of which could be used in this design.

The MRI noise issue was a serious one, and it caused the failure of both of the low fidelity prototypes that were constructed before the start of this design project. The methods used to circumvent this issue are explained in detail in the engineering analysis section.

Shielding

Shielding against high frequency RF noise was achieved using the methods described in the shielding analysis and design section. However, shielding against the low frequency magnetic noise described in Figure 8 was much more difficult to consider. Traditional magnetic shields use magnetic alloys to redistribute the magnetic field lines [17]. However, since magnetic and ferrous materials aren't allowed in devices for use in MR environments, this option was not considered. Because of this, magnetic shielding was not achievable.

Another challenge was designing a shield that would be compatible with all MRI systems. The Larmour frequency of the MRI scanner refers to the rate of precession of magnetic moment of the proton around the external magnetic field. This frequency is used to calculate the skin depth and is related to the magnetic field strength [22]. As the magnetic field strength decreases, the Larmour frequency decreases, and as Equation 1 shows, the skin depth would increase thus requiring a thicker shield. This challenge was overcome by using a shield thickness that is a magnitude higher than the skin depth, such that the shield would be effective for various magnetic field strengths.

4.3 Design Prototype

The prototype is an electrical component that amplifies the output of the Transpac IV blood pressure sensor and transmits it to the operator console in the MRI scan room.

This prototype revision used an off-the-shelf lab power supply and an oscilloscope to visualize the blood pressure waveform. Future revisions of this device will use an integrated medical power supply and a receiver module with an analog to digital converter and micro-controller will replace the oscilloscope.

5

Design Testing and Evaluation

Four tests were conducted on this prototype. The first two would test how the design handles the electrical noise emitted by the MRI scanner while running. The first test would deem the prototype successful if the peak to peak baseline noise measurement was constant during many different scanning scenarios. The second would deem the prototype successful if the blood pressure of the animal patient was successfully captured on the oscilloscope for the duration of the scan and if this reading had no detectable instances of measurement error. The third test would ensure that the prototype can withstand the high acoustic noise emitted by the MRI scanner. This would deem the prototype successful if the output showed no detectable instances of measurement error due to acoustic noise. Finally, the fourth test would deem the prototype successful if it showed no measurement attenuation for the different catheter lengths used in this research.

5.1 Testing Procedures and Results

Test I: System Noise Floor Measurement

The transducer was primed and zeroed exactly as it would be in a clinical setting, and then loaded with a static pressure source (a graduated cylinder filled with water) to approximately 15 mmHg. The baseline measurement was recorded, and then the MRI scanner was operated at it's maximum output power of 16 kW. An oscilloscope was used to measure the MRI scanner's effect on the amplifier's output waveform. This test was iteratively repeated at distances of 1 m, 2 m, and 5 m from the MRI scanner's bore, where 1 m was the minimum possible distance (constrained by IV pole placement) and 5m was edge of the scan room, just beyond the MRI scanner's 5 Gauss radius. This test was also repeated using both a shielded and unshielded transducer.

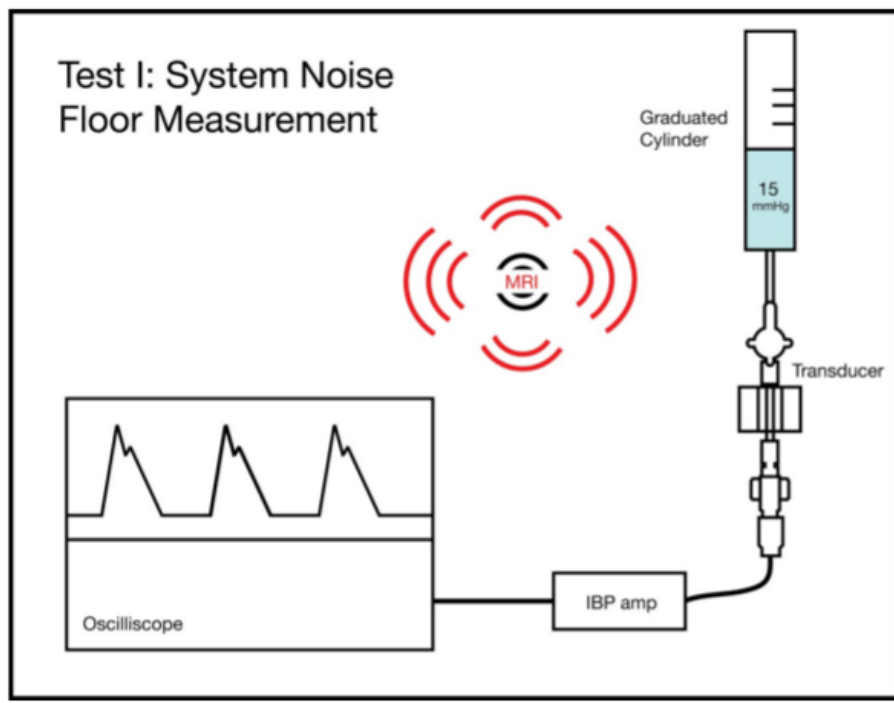


Figure 16: System noise floor test plan schematic.

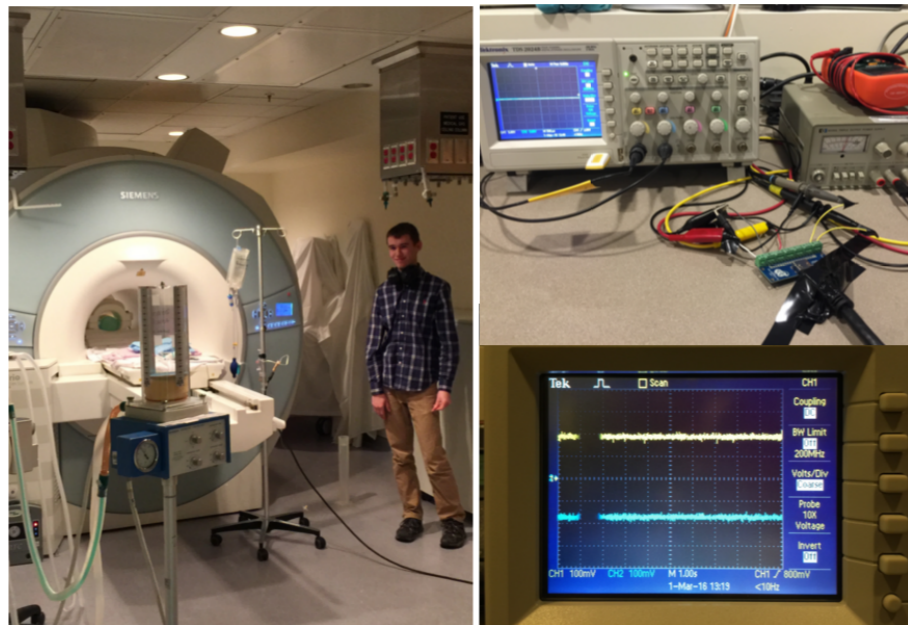


Figure 17: System noise floor testing setup.

As shown in the bottom right photograph of Figure 17, the total system noise with the MRI scanner operating varied from 5-15 mV peak to peak noise during the worst case measurement conditions of the scanner transducer distance of 1m, using an unshielded transducer. During the iterative repetitions of this test under different conditions, all of the configurations exhibited the same 5-15 mV noise, so we concluded that this was the noise floor of our system during scanner operation.

Test II: Clinical Conditions Test

The transducer was primed and set up identically to the configuration used in Test I. Next the pressure port of the Transpac IV transducer was connected to a rigid cannula which was inserted into a Yorkshire pig's carotid artery. The blood pressure was measured using an oscilloscope on roll mode for 2.5 hours, while a large variety of MRI scans were run at the scanner's maximum output power.

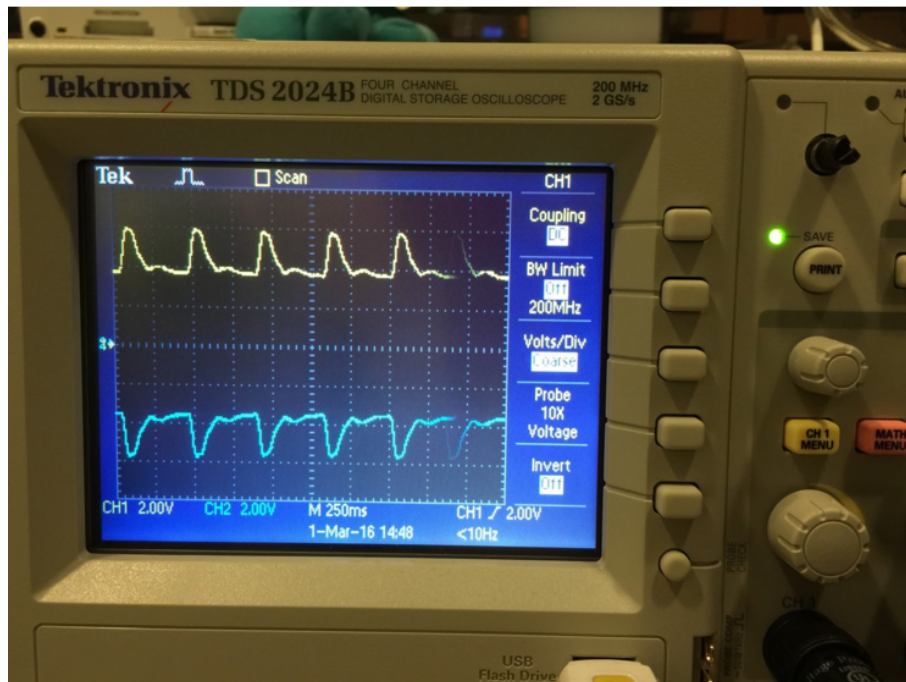


Figure 18: Invasive blood pressure trace recorded on a Yorkshire pig.

The measurement system operated perfectly throughout the entire scan, with no detectable instances of measurement error induced by electromagnetic interference, baseline drift or distortion. Additionally, the five MRI experts present were not able

to identify any imaging artifact induced by the IBP measurement system. As a point of comparison, the Siemens EEG monitor, which was being used throughout the experiment to monitor the animal's vital signs, failed seven times throughout the MRI scans, because of MRI scanner interference. Another point of comparison was provided by the InVivo cardiac monitor which the veterinary technicians used to monitor the animal's vital signs throughout the experiment. The InVivo monitor's readings for heart rate were identical to the IBP system's measurements throughout the entire test. Based on these results, we conclude that the IBP measurement system prototype is MRI compatible, and functions sufficiently reliably to be adapted into a product for the MRI research market.

Test III: Enclosure Acoustic Testing

Acoustic testing was performed on an unshielded transducer to determine the effects of sound waves on the transducer. This was done in preparation of the MRI scanner emitting high amplitude sound waves during operation. A low fidelity test was performed in which a speaker was placed right beside the transducer at full volume to see if there was any noise pickup that would affect the blood pressure signal.

MRI-related acoustic noise is produced when induced Lorentz forces cause motion or vibration of the gradient coils which impact their mountings. This noise is affected by many parameters such as the pulse sequence, system hardware, and external environment. Various tests have been done to show that MR systems with ranging base magnetic field strengths have MR-related imaging sound levels between 84-131 dB [23]. A study by Brummett et al. reported that 43% of MRI patients who had no hearing protection or improper hearing protection suffered temporary hearing impairments [24].

The Bose SoundLink III speaker used for this test has a sound power rating of 90 dB at a distance of 1m at full volume [25]. The speaker was placed at a distance of about 10 cm from the transducer and multiple songs of different bass compositions were played at full volume. It is assumed that since the speaker is closer than 1 m, the sound power simulated will be greater than 90dB during the test, simulating a

similar sound level to the systems noted above.

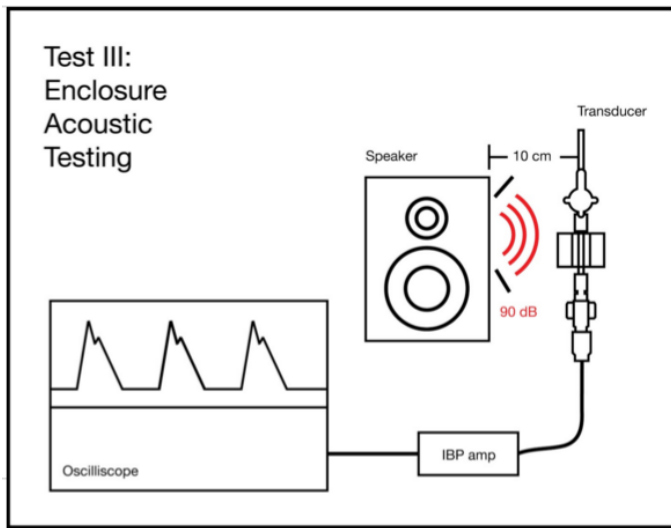


Figure 19: Enclosure acoustic test plan schematic.

Overall, there were no noticeable changes to the blood pressure signal during any point in the experiment. The noise, if any, created from the sound waves emitted from the speaker is considered negligible. Based on the results of this simple test, acoustic shielding for the transducer was considered unnecessary.

Test IV: Rigid Cannula Attenuation Testing

To test the pressure attenuation of the invasive blood pressure catheter, two identical pressure transducers were connected in series. One transducer was placed as the pressure source (a standard hypodermic syringe), and the other was placed at the opposite end of an invasive blood pressure measurement tube as shown in Figures 20 and 21.

Tubing lengths of 1 m and 4 m were tested and produced similar results to the simulation. Pressure waveforms in the frequency range of interest were generated by pressing and pulling on the syringe. The attenuation was so low that it was immeasurable using these transducers.

Based on the results of this test, it was concluded that pressure loss was a non-issue for use with the type of tubing and lengths typically used in preclinical research

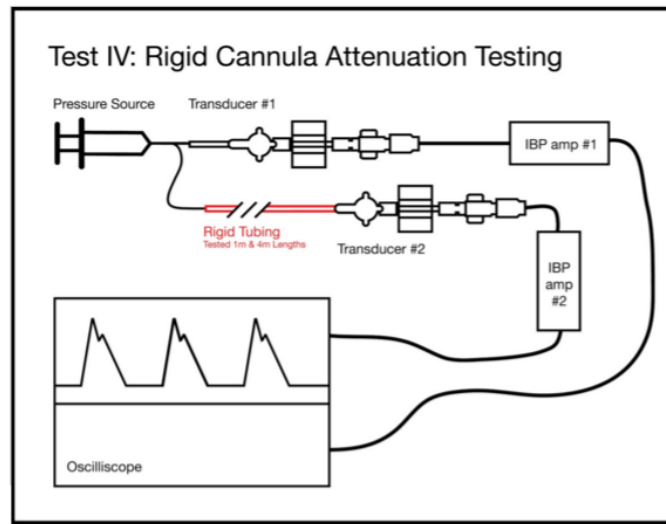


Figure 20: Rigid cannula attenuation test plan schematic.

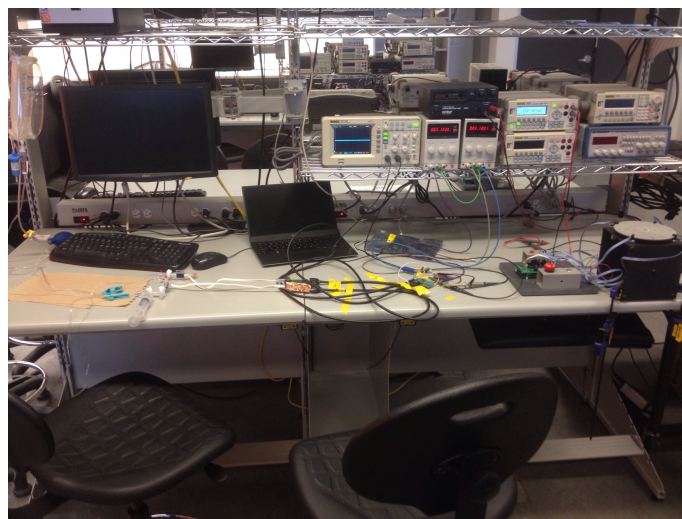


Figure 21: Photograph of the line loss testing setup.



(a) Pressure signal in frequency of interest

(b) Pressure signal outside of frequency of interest

Figure 22: Experimental results of pressure loss with 4m of tubing

in MRI.

5.2 Discussion

Test I showed that the system has an excellent signal to noise ratio, which means that unlike most commercially available systems, this measurement system will retain its accuracy when used in the MRI environment.

Test II proved that the system is ready for preclinical research use, because the system worked reliably throughout the entire animal experiment.

Test III showed that acoustic noise does not have a measurable effect on the Transpac IV transducer, confirming that the high volume acoustic noise emitted by the MRI during some types of MRI protocols will not cause intermittent measurement errors.

Test IV confirmed the results of the acoustic model, proving that the tubing lengths used in this system will not introduce significant measurement error.

Some specifications were not tested, because of time constraints. Future testing will include testing of the system's absolute measurement accuracy, testing of the system's typical setup time, and testing of the amount of time required to take down and clean the system.

6

Recommendations

The IBP measurement system prototyped here met or exceeded all of the key specifications for use in MRI, thus the project is deemed to be successful. The system will be used as-is during a series of preclinical MRI trials at SickKids in a series of animal trials and tests on mechanical heart models.

6.1 Circuit Design Revisions

Now that an accurate and reliable analog input stage has been designed, other aspects of the circuitry could be revised and simplified to reduce the cost of the system. In the first revision, precision components were used throughout, where lower cost alternatives could have been applied in some instances without compromising the system accuracy. For example, the LT1167A is a spectacular input amplifier, but in this application the bog standard AD620 would have been sufficiently accurate.

Another way the system could be simplified and improved would be incorporating an analog to digital converter onto the same PCB as the analog amplifier, and using digital communications throughout. This approach would eliminate the need for the relatively expensive analog cable driver circuitry and reduce system cost, because the receiver end would consist of nothing more than a generic micro-controller.

6.2 Human Factors Considerations

Human factors and ergonomic analysis could be applied to make this system easier to use. These considerations include:

1. Optimizing the cognitive ergonomics of the system setup, providing attachments and enclosures that make system setup as simple as possible, discouraging the most common or most dangerous errors.

2. Optimizing the cognitive ergonomics of the blood pressure readout interface, ensuring that technicians, veterinarians, and MRI scientists can all access the respective information that they need as easily as possible.
3. Optimizing the cognitive ergonomics of the system's instructions, ensuring that there are as few steps as possible and that the information is presented clearly.

6.3 Expansion of System Capabilities

Several useful measurement features could be added to the measurement system for convenience including:

1. Adding multi-channel measurement capabilities, so that atrial and ventricular pressures could be monitored simultaneously.
2. Building signal converters to the make the measurement unit compatible with standard physiological monitors.
3. Designing and implementing a software application to allow MR technologists to monitor and log the pressure measurements, complete with annotation capability for marking the beginning and ending of each MRI scan.
4. Capturing and displaying the systolic and diastolic pressures in software for use by the veterinary staff.

7

Conclusion

The IBP measurement system prototype met or exceeded all of the specifications for general animal research use in MRI, thus the project was successful. A slightly revised version of this system will be used during a series of preclinical MRI trials on animals at SickKids and tests on mechanical heart models. This project has received additional funding to cover the costs of building additional units, expanding the system's capabilities, and publishing the design in an MRI instrumentation journal.

8

Project Management

8.1 Team Member Roles

Sarah Cook took on the roles of acoustics researcher and project manager. Matt Jones worked on mechanical design, manufacturing engineering and performed research on transducer shielding and the effects of MRI gradient noise on the circuitry. Isaac Hunter assisted with circuit design and manufacturing. Josh Bradshaw was the lead electronics designer and co-ordinated with SickKids to determine user requirements and do system testing.

8.2 Schedule and Intermediate Deadlines

The schedule of this project was based on the dates that SickKids had available for testing the system in MRI. The only two possible dates were March 1 and March 29, so the team opted to finish a minimal prototype by March 1.

Table 7: Project Schedule

Jan 20	Circuit Design Complete
Jan 25	PCB design complete
Feb 5	Prototype I assembled
March 1	Prototype I ready for testing at SickKids
March 12	Acoustic model complete
March 15	Acoustic model testing setup complete

All of the above deadlines were met, so no further project management was required.

Appendix A: User Personas

General Information

Brian Courtney (46, M)

Primary User – Surgeon / Scientist

Invested in development of an improved technology

Will be the user activating and monitoring the device



Main Characteristics

- Hard working
- Passionate about helping others
- Patient
- Part of the research team developing the device
- Works with grad students and coops to improve device performance

Current Technology Use

- Engineering and medical degrees from Stanford
- Regular use of medical devices
- Responsible for cleaning the devices used in animals
- Has previous experience with primitive prototypes

Needs & Desires

- Device should not interfere with operation
- Ability to be cleaned easily
- Cords are contained neatly
- User interface on patient monitor is intuitive
- Device is accurate to the normal standards
- Minimal apparatus

User Goals

- Effective in measuring blood pressure
- Blood pressure is accurate
- Wants device calibrated before procedure
- Wants all the parts of the device sterile
- Device can be kept sterile

Current Pains

- There is only a single device on the market which is expensive
- Would prefer to do surgeries not in MRI suite
- Sometimes has to wait for the device to be calibrated
- Cables can be messy making them a tripping hazard

Scenario

- Brian will use the device to do gating during an animal experiment. He has sufficient surgical training to place a catheter, so he will do the operation himself in the clinical room of the MR suite, and then place the animal in the MRI.

General Information

Marc Lukacs (34, M)

Secondary User – MRI system operator

Would like the device to be easy to calibrate and clean

Will be the user setting up, calibrating, and cleaning the device



Main Characteristics

- Often rushed
- Efficient problem solver
- Quick to react to issues with the system
- Considers himself the decision maker
- Enjoys all the challenges that MRI imaging brings

Current Technology Use

- Knowledgeable about all things MRI
- Can set up and calibrate all kinds of MRI tech.
- Is the one performing the MRI scan
- Monitors the patient monitor for abnormalities in blood pressure

Needs & Desires

- Would like as little calibration as possible
- Wires should be contained (Marc is in and out of the MRI suite often)
- Device doesn't interfere with MRI scanner performance

User Goals

- Quick setup time
- Setup is easy to learn and remember
- Device works without constant intervention
- Accidents involving cables are minimized

Current Pains

- Often tight on time as it is
- Calibration takes longer than ideal
- Too much wiring across the MRI suite (from all devices)
- Doesn't like that it has to be attached to the scanner bed

Scenario

- An animal experiment has been scheduled. Marc must initialize the MRI suite then set up and calibrate the IBP device. There is a small issue with the ventilator that Marc must fix before beginning the scan, so his attention is already divided. Time is very limited because the team has a very short MRI booking for this experiment.

Appendix B: Pressure Attenuation Code

```
1 - u = .001002; % dynamic viscosity of water
2 - a = 0.0000024; %cross-sectional area of tubing
3 - d = 0.0019; %diameter of tubing
4 - B = 2190000000; %bulk modulus of water
5 - D = 998.2; % density of water
6 - Po = 16000; %initial pressure
7 - T = 0.8; % period of blood pressure wave
8 - w = 2*pi/3.14/T;
9 - t=0.000006748;
10 - P = [];
11 - Z = [];
12 - T = [];
13 - G = [];
14 - for z = 0:0.1:150
15 -     Rdot = 32*u/(a*d^2);
16 -     Gdot = (a*d^2)/(32*u*z^2);
17 -     Cdot = a/B;
18 -     Ldot = D/a;
19 -
20 -     gamma = sqrt((Rdot + 1i*w*Ldot)*(Gdot + 1i*w*Cdot));
21 -     alpha = real(gamma);
22 -     beta = imag(gamma);
23 -
24 -     p = Po*exp(alpha*z);
25 -     %p = Po*exp(-alpha*z) *cos(w*t - beta*z) + Pi*exp(alpha*z)*cos(w*t + beta*z);
26 -     P = [P p];
27 -     Z = [Z z];
28 -     T = [T t];
29 -     G = [G gamma];
30 -     t = t + 0.000006748;
31 - end
32 - plot(Z,P);
```

References

- [1] Bishop, J. *Retrospective gating for mouse cardiac MRI*. Magnetic Resonance in Medicine. 55(3), 472–7 (2006).
- [2] *T2-weighted Fourier velocity encoding: in vivo vascular MR oximetry*. SickKids Fetal MRI, Press Release. Accessed at: <http://www.sickkids.ca/Research/fetalMRI/T2-weighted/index.html> (2015).
- [3] Zong W. et al. *An open-source algorithm to detect onset of arterial blood pressure pulses*. Computers in Cardiology, 259–262 (2003).
- [4] *MAGNETOM Trio a Tim System*. Siemens, Operator Manual - MR System (2009).
- [5] Woods, T. O., *Standards for medical devices in MRI: present and future*. Journal of Magnetic Resonance Imaging: JMRI, 26(5), 1186–9, 2007.
- [6] *Samba Preclin Samba 200 Product Presentation Samba Preclin 420 / 360 Transducer*. Samba Precilin, (2013).
- [7] Pidac, *Best Practices for Cleaning , Disinfection and Sterilization of Medical Equipment / Devices*. Magnetic Resonance Imaging, 2013. (2013).
- [8] Garreffa, G., Carn, *Real-time MR artifacts filtering during continuous EEG/fMRI acquisition*. Magnetic Resonance Imaging, 2003.
- [9] Horowitz, P., Hill, W. *The Art of Electronics 3rd Edition*. Cambridge University Press, 299. (2015).
- [10] *LT1167A Datasheet*. Linear Technologies, Datasheet (2015).
- [11] Moshe Gerstenhaber, *Reducing RFI Rectification Errors in In-Amp Circuits. Analog Devices*, Application Note.

- [12] *Transpac IV Disposable Pressure Transducer*. ICU Medical, Transpac Sell Sheet (2012).
- [13] *Use of Transpac Transducer Devices in MRI.* ICU Medical, Application Note, (2015).
- [14] Wm, B., Klein, *Improve Instrument Amplifier Performance with X2Y ® Optimized Input Filter*. Johnson Dielectrics, Application Note, 2015.
- [15] Moshe Gerstenhaber, *High-Definition Multimedia Interface Specification 1.3a*. Philips Consumer Electronics, International.
- [16] Bruce Carter, *How (Not) to Decouple High-Speed Operational Amplifiers*. Texas Instruments, Application Note, September 2001.
- [17] *EMI, RFI, and Shielding Concepts*. Analog Devices Application Note.
- [18] K. Blattenberger, *Skin Depth (aka Skin Effect)*. RF Cafe, 2016. [Online]. Available: <http://www.rfcafe.com/references/electrical/skin-depth.htm>. [Accessed: 17-Mar- 2016].
- [19] *An Open-Source Hardware and Software System for Acquisition and Real-Time Processing of Electrophysiology during High Field MRI*. Journal of Neuroscience, 175(2), 165–186. (2010).
- [20] J. M. Kirshner *Design Theory of Fluidic Components* Academic Press, January 28, 1975
- [21] J. S. Ansari *Propagation of Disturbance in Fluid Lines* Journal of Basic Engineering 89(2), 415-422. (Jun 01, 1967)
- [22] J. Jones, *Larmor Frequency*. Radiopaedia, 2016. [Online]. Available: <http://radiopaedia.org/articles/larmor-frequency>. [Accessed: 16- Mar- 2016].
- [23] F. Shellock. *Acoustic Noise and MRI Procedures*. MRI Safety. 2016. [Online]. Available: <http://www.mrisafety.com/SafetyInfov.asp?SafetyInfoID=252>. [Accessed: 10- Mar- 2016].

- [24] R. Brummett, J. Talbot and P. Charuhas. *Potential Hearing Loss Resulting from MR Imaging*. Radiology, 169(2). (1988).
- [25] *The Loudest Portable Speakers Review - Best of 2016*. Loudest Portable Speakers. 2016. [Online]. Available: <http://loudestportablespeakers.com/>. [Accessed: 10-Mar- 2016].